SF2A 2023
M. N'Diaye, A. Siebert, N. Lagarde, O. Venot, K. Baillié, M. Béthermin, E. Lagadec, J. Malzac, J. Richard (eds)

MEV-GEV POLARIMETRY WITH THE FERMI-LAT: A FIRST SENSITIVITY ESTIMATE

A. Laviron[1], D. Bernard[1] and P. Bruel[1]

Abstract. A measurement of MeV-GeV linear polarization would provide information about the emission mechanisms of gamma-ray sources, especially pulsars and AGNs (active galaxy nuclei). The *Fermi* Large Area Telescope (*Fermi*-LAT) detects gamma rays between $\sim 20\,\mathrm{MeV}$ and $\sim 300\,\mathrm{GeV}$, using their conversion into an electron-positron pair, with the linear polarization affecting the distribution of the azimuthal direction of the pair. Measuring this azimuthal direction is extremely challenging due to the multiple scattering of the electron-positron pair in the detector. We present the current effort to extract the polarization information from the *Fermi*-LAT data, including recent developments on the simulation implementation and the event reconstruction and selection. This allows us to estimate the expected sensitivity to linear polarization of the *Fermi*-LAT, and we apply this to the Vela pulsar.

Keywords: Gamma-ray, Polarimetry, Pulsar

1 Introduction

Pulsars were discovered in 1967 as pulsating radio sources Hewish et al. (1968). They were quickly interpreted as magnetized, rotating neutron stars. The *Fermi* Large Area Telescope reported 294 pulsars detected in the GeV range*, making pulsars a significant fraction of the known gamma-ray sources. Their gamma-ray emission has a spectral shape of a power-law with sub-exponential cutoff at an energy of a few GeV (Smith et al. 2023). If the radio emission is thought to originate from the polar cap, the gamma-ray emission cannot escape that part of the magnetosphere because of the $\gamma - B \rightarrow e^+e^-$ absorption by the intense magnetic field (Abdo et al. 2010). The gamma-ray emission therefore comes from an outer part of the magnetosphere, but the exact location of that emission region and the radiative processes at play are still debated. The polarization signature of these different emission processes and emission regions differ significantly (Harding & Kalapotharakos 2017), with curvature radiation emitted within the light cylinder predicted to be more polarized than synchrotron emission from the striped wind.

In the MeV to GeV energy range, the dominant interaction process of gamma rays with matter is $e^+ - e^-$ pair production. This process is inherently sensitive to linear polarization: the bisector φ of the azimuthal angles of the electron and positron is preferentially perpendicular to the polarization direction, as can be seen in Figure 1 (left). The φ distribution, called in the following "polarigram", therefore has a cosine modulation, as can be seen in Figure 1 (right). One of the minima of the polarigram is the polarization angle φ_0 and the amplitude of the modulation A is proportional to the polarization fraction P,

$$\mathrm{P} = A/A_{100}\ , \tag{1.1}$$

where A_{100} is the modulation of a 100 % polarized source.

The *Fermi*-LAT (Atwood et al. 2009) is a gamma-ray space telescope, using pair production and observing in the $\sim 20\,\mathrm{MeV}$ to $\gtrsim 300\,\mathrm{GeV}$ energy range. It is composed of two main subsystems: a tracker to measure the direction of the incoming gamma ray and a calorimeter to measure its energy. It was designed to optimize the effective area and angular resolution throughout its energy range, but not its polarization sensitivity. Previous polarimetry attempts using information provided by the standard *Fermi*-LAT reconstruction were not

[1] Laboratoire Leprince-Ringuet, CNRS/IN2P3, Ecole polytechnique, Institut Polytechnique de Paris, 91120 Palaiseau, France
*https://confluence.slac.stanford.edu/display/GLAMCOG/Public+List+of+LAT-Detected+Gamma-Ray+Pulsars

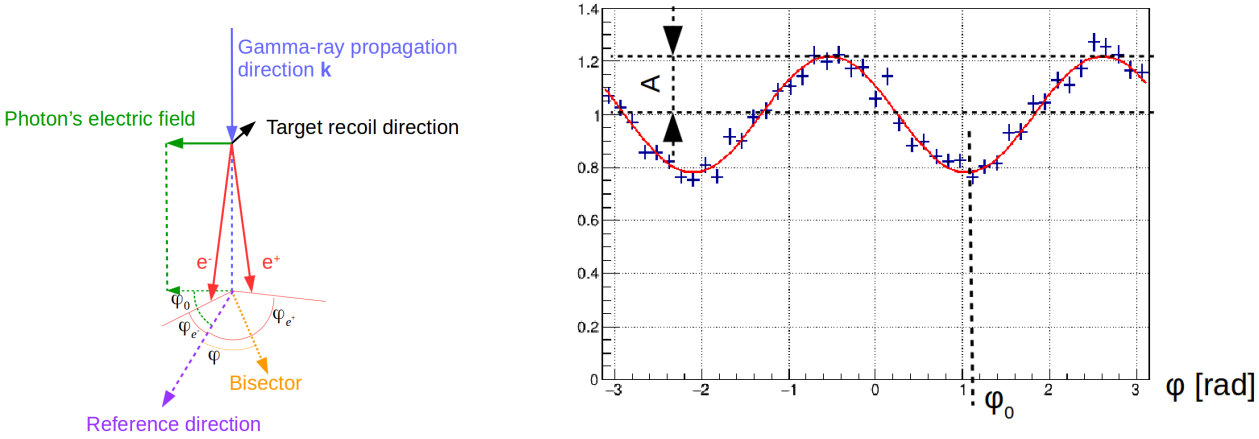

Fig. 1. Left: diagram of pair production. Right: distribution of φ angles, called a polarigram. The distribution minimum φ_0 is the polarization angle, the amplitude A is related to the polarization fraction.

successful (Giomi et al. 2017). Here we present a new approach to *Fermi*-LAT polarimetry based on the work of Bernard (2022). It relies on a dedicated event reconstruction that is described in Section 2. To develop this method, we performed Monte-Carlo simulations of the full LAT detector using Gleam (Atwood et al. 2009), a simulation software based on Geant4 (Agostinelli et al. 2003). The physics list of the Geant4 simulation has been modified to use the 5-dimensional, polarized Bethe-Heitler gamma-ray conversion model (Bernard 2018). Section 3 presents the results and a preliminary polarization sensitivity estimate applied to the Vela pulsar.

2 Methodology

The *Fermi*-LAT tracker is composed of 4×4 towers. Each tower contains 18 detector layers, each layer being composed of two single-sided silicon strip detectors, one dedicated to the measurement of the x coordinate and the other to the y coordinate†. For that purpose, they are electrically segmented along one direction with strips separated by 0.228 mm. The top 12 layers have a thin tungsten converter (3.5 % radiation length, 0.1 mm) and compose the Front section of the tracker. The Back section of the tracker consists of 4 layers with a thicker tungsten converter (18 % radiation length, 0.72 mm). The *Fermi*-LAT standard event reconstruction algorithm, named Pass 8 (Atwood et al. 2013), first groups contiguous strips that triggered into clusters in each silicon plane. Then it combines clusters to form tracks that are fitted to extract their direction. Next, it chooses the best track, that we call "the Pass 8 track" in the following, to reconstruct the incident gamma-ray direction.

The main challenge in pair-production polarimetry is the multiple Coulomb scattering of the electron and positron by the detector material, especially near the gamma-ray conversion point. Multiple scattering increases with the amount of material crossed. Therefore, as was found in Bernard (2022), the azimuthal angle can be computed from the first two layers of the event, the conversion layer and in the layer just below the conversion layer, called hereafter the "layer below conversion". Within the detector layer, the conversion happens either in the silicon detectors or in the tungsten converter, where multiple scattering is greater. By construction, the Pass 8 reconstructed z conversion coordinate is located in either the upper or lower silicon detector of the conversion layer. The majority of "upper detector" events are tungsten conversions. "Lower detector" events represent only 5.5 % of all events at 100 MeV, but 76 % of them are silicon conversions, expected to be much more sensitive to polarization. We will therefore report their measured modulation amplitudes separately.

In order to compute a pair azimuthal angle from the cluster information, we need one point in the conversion layer, and two points (corresponding to the crossing points of the electron and positron) in the layer below conversion. We select events that have at least one cluster (in either x or y) and at most one cluster in x and one cluster in y in the conversion layer. In the layer below conversion, we use events that have two clusters in either x or y and either one or two clusters in the other direction. This leads to two configurations that are shown in Figure 2. We name them according to their number of possible azimuthal angles (NPAA). The one schematized in Figure 2 (left) is called NPAA1. It has two x coordinates for the electron and positron

†In the LAT frame, the x and y axes span the silicon detectors plane and the z axis points towards the LAT boresight.

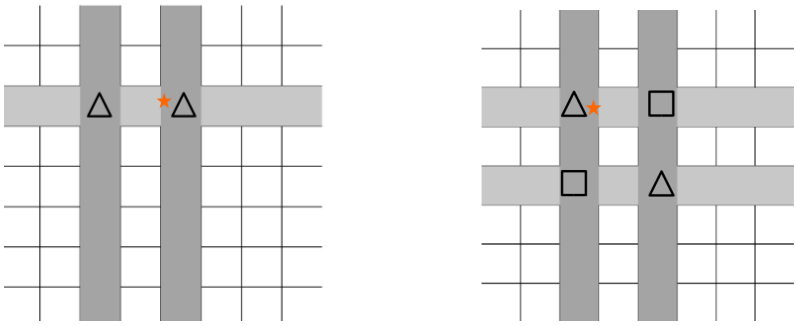

Fig. 2. Cluster configurations in the layer below conversion. Light grey represents the y clusters and dark grey the x clusters. The orange star represents the coordinates of the Pass 8 track in that plane. The black triangles and squares represent the sets of (x, y) positions that we may use to compute an azimuthal angle. Left: NPAA1 (there is one cluster in either x or y). Right: NPAA2 (there are two clusters in both x and y, yielding two possible azimuthal angles).

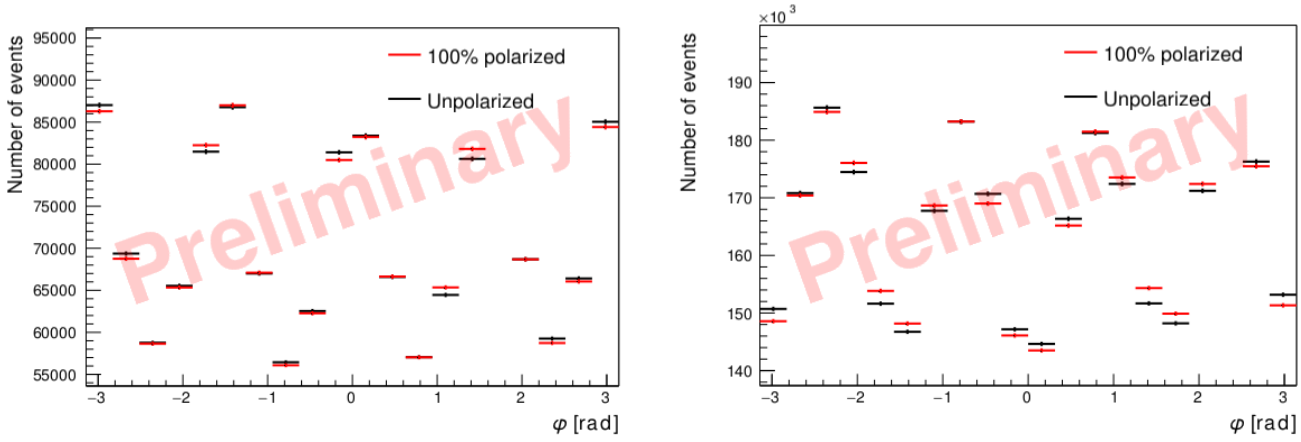

Fig. 3. Distribution of φ azimuthal angles, for a 100 % polarized source in red and a 0 % polarized source in black. Only Front-converted and upper detector events are shown. Left: distribution for NPAA1 events. Right: NPAA2 events.

and a single y coordinate, leaving a single possible pair azimuthal angle, computed using the coordinates in the conversion layer and the two xy coordinates indicated by black triangles. The event configuration shown in Figure 2 (right) has two x coordinates and two y coordinates. This results in an ambiguity: we could compute an azimuthal angle using either the two coordinates indicated by the black triangles or by the black squares. We therefore call these events NPAA2. In that case, we use the azimuthal angle computed from the pair possibility that is closer to the Pass 8 track.

3 Results

In order to estimate the *Fermi*-LAT sensitivity to polarization, we first measure the modulation amplitude A_{100} (defined in Eq. 1.1) for each event configuration. To do so, we simulate gamma rays from the celestial coordinates of the Vela pulsar (J2000 R.A. = 128.84 °, Dec = − 45.18 °). Simulations are performed at three energies: 50 MeV, 100 MeV and 200 MeV. For each energy, we simulate an unpolarized source (0 % polarized), and a fully polarized source (100 % polarized, polarization angle of 0 °). Figure 3 shows examples of polarigrams, for 100 MeV, Front-converted and "upper detector" events, NPAA1 (left) and NPAA2 (right). These distributions do not show the cosine modulation because they are dominated by the x-y structure of the LAT tracker.

Ratios (bin-to-bin) of the polarized distribution to the unpolarized distribution are shown in Figure 4. For the sake of simplicity, we refer to these ratios as polarigrams. We fit these ratios with a cosine function to extract the modulation amplitudes A_{100}. The amplitudes of Front, upper detector events are 0.77 ± 0.16 % for NPAA1 events and 1.20 ± 0.11 % for NPAA2 events (respectively 1.72 ± 0.35 % and 2.54 ± 0.35 % for Front, lower detector events). We observe that modulations of NPAA1 events are smaller than those of NPAA2 events, because the

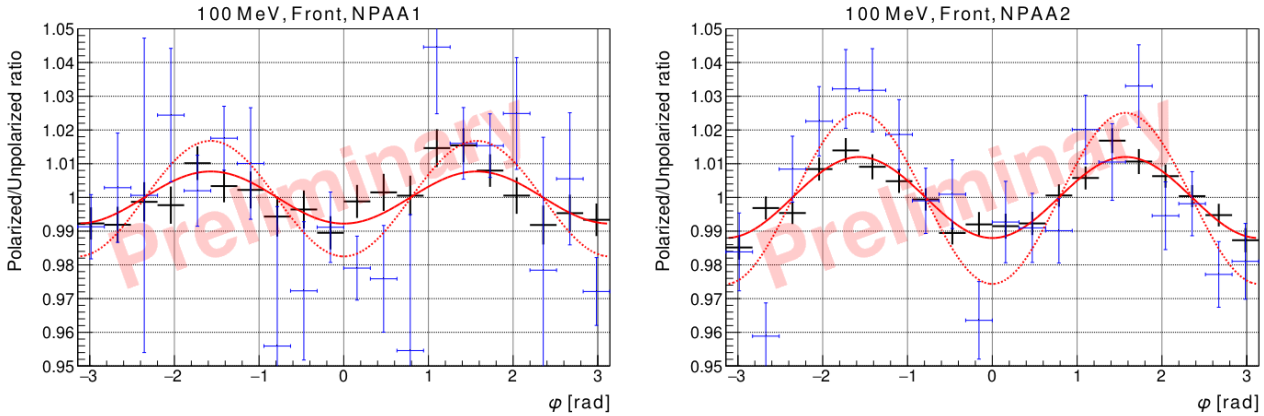

Fig. 4. Polarigrams of Front-converted events at 100 MeV. Thin blue line (fitted by red dashed line): "lower detector" events. Thicker black line (fitted by red continuous line): "upper detector" events. Left: NPAA1. Right: NPAA2.

azimuthal angles reconstructed in NPAA1 events are less precise. As expected, the "lower detector" events are much more sensitive to polarization. Finally, the modulation of Back events (not shown here) is compatible with zero. These overall low numbers are not surprising since the LAT was not designed for polarimetry. The modulation amplitudes vary slightly with energy. These results are comparable with those obtained with a simplified model of the *Fermi*-LAT in Bernard (2022). Our simulations at 50 MeV, 100 MeV and 200 MeV are at the center of three logarithmic energy bins in the range 35 MeV to 283 MeV. In that energy range, the observed Vela pulsar count spectrum is almost flat, and the expected number of photons is $\sim 2 \times 10^6$ for 15 years of observation. Under these assumptions, we obtain an uncertainty on the measured linear polarization fraction of $\sigma_{\rm P} \simeq 20\,\%$.

4 Conclusions

We have presented a new analysis that allows us to obtain for the first time a non-zero sensitivity to linear polarization with *Fermi*-LAT. This result is enabled by directly using the tracker cluster information rather than the output of the standard event reconstruction. Using simulations, we measure modulation amplitudes up to 2.5 % in the energy range between ~ 30 MeV and ~ 300 MeV and estimate the expected sensitivity to the linear polarization of the Vela pulsar to be about 20 % with 15 years of data. The next step of this study is to extend the investigated energy range. We will then apply the analysis to *Fermi*-LAT data.

The *Fermi*-LAT Collaboration acknowledges support for LAT development, operation and data analysis from NASA and DOE (United States), CEA/Irfu and IN2P3/CNRS (France), ASI and INFN (Italy), MEXT, KEK, and JAXA (Japan), and the K.A. Wallenberg Foundation, the Swedish Research Council and the National Space Board (Sweden). Science analysis support in the operations phase from INAF (Italy) and CNES (France) is also gratefully acknowledged. This work performed in part under DOE Contract DE-AC02-76SF00515.

References

Abdo, A. A., Ackermann, M., Ajello, M., et al. 2010, ApJS, 187, 460.

Agostinelli, S., Allison, J., Amako, K., et al. 2003, Nucl.Instrum.Meth., 506, 250.

Atwood, W. B., Abdo, A. A., Ackermann, M., et al. 2009, ApJ, 697, 1071.

Atwood, W., Albert, A., Baldini, L., et al. 2013, arXiv:1303.3514.

Bernard, D. 2018, Nucl.Instrum.Meth., 899, 85.

Bernard, D. 2022, Nucl.Instrum.Meth., 1042, 167462.

Giomi, M., Bühler, R., Sgrò, C., et al. 2017, 6th International Symposium on High Energy Gamma-Ray Astronomy, 1792, 070022, arXiv:1610.06729.

Harding, A. K. & Kalapotharakos, C. 2017, ApJ, 840, 73.

Hewish, A., Bell, S. J., Pilkington, J. D. H., et al. 1968, Nature, 217, 709.

Smith et al. ApJS submitted (2023), arXiv:2307.11132.